Electronic structure of clean and hydrogen-chemisorbed Ge(001) surfaces studied by photoelectron spectroscopy

Erik Landemark, C. J. Karlsson, L. S. O. Johansson,* and R. I. G. Uhrberg
Department of Physics and Measurement Technology, Linköping Institute of Technology, S-581 83 Linköping, Sweden
(Received 4 November 1993)

The electronic structure of the clean and the hydrogen-chemisorbed Ge(001) surface has been studied with photoelectron spectroscopy. Angle-resolved valence-band and high-resolution core-level spectra were recorded for both the room-temperature, 2×1, and the low-temperature, $c(4\times2)$, reconstructions of the clean surface. The electronic structure for the two phases was found to be very similar. The Ge $3d$ core-level spectra are decomposed with two surface-shifted components and the different origins of the components are discussed. The valence-band electronic structure of the clean, room-temperature, 2×1 and the hydrogen-induced 2×1:H reconstructions has been studied in detail by polarization-dependent angle-resolved photoemission. The surface-state dispersions $E(\bar{k}_{\parallel})$ in the [010] and [110] directions are mapped out. For the clean surface these dispersions are compared with surface-state bands obtained from a self-consistent calculation, using the local-density approximation and scattering theory, applied to a semi-infinite crystal with a 2×1 reconstructed surface consisting of asymmetric dimers. In spectra recorded from freshly annealed samples a structure is observed just above the Fermi level. This structure can be explained by thermal excitation to an empty dangling-bond band. The valence-band maximum was determined to be less than 0.1–0.2 eV below the Fermi-level for the clean 2×1 surface. On the hydrogen-chemisorbed 2×1:H surface two strong hydrogen-induced surface states are observed in the energy region 4.4–5.5 eV below E_F. The symmetry properties of these states, investigated by their polarization dependence, were found to be similar to the two corresponding states of the monohydride Si(001)2×1:H surface.

I. INTRODUCTION

Both the Ge(001) and Si(001) surfaces are terminated by dimers which constitute the basic 2×1 building blocks of the surface reconstructions.[1] The 2×1 low-energy electron-diffraction (LEED) pattern observed at room temperature (RT) transforms at low temperature to a $c(4\times2)$ pattern for both these surfaces. The $c(4\times2)$ reconstruction is explained by asymmetric dimers with alternating buckling directions, arranged in an antiferromagnetic manner.

The detailed structure of the dimers on the Si(001) surface at RT, i.e., whether the dimers are symmetric or asymmetric, has been a question under debate for a long time, which to a high degree is motivated by the symmetric appearance of the dimers in scanning tunneling microscopy (STM) studies (see discussion in Refs. 2 and 3). Very recently photoemission[2] and STM,[3] both performed at RT and 120 K, have provided evidence for asymmetric Si dimers at RT. In the low-temperature STM images the number of buckled dimers increased at the expense of symmetric-appearing dimers. It was concluded that, at room temperature, the dimers are thermally activated and that their buckling direction switches, leading to the symmetric appearance in the STM images.

In STM studies of the Ge(001)2×1 surface performed at RT, asymmetric dimers arranged in local $c(4\times2)$ and $p(2\times2)$ regions are observed.[4] The picture of asymmetric dimers for Ge(001) is supported by He diffraction by Cardillo and co-workers,[5] He^+-ion scattering by Culbertson, Kuk, and Feldman,[6] x-ray diffraction by Rossmann *et al.*,[7] and self-consistent total-energy and electronic-structure calculations by Needels, Payne, and Joannopoulos[8] and Krüger *et al.*,[9] respectively.

For both Si(001) and Ge(001) well-ordered 2×1:H reconstructed (monohydride) surfaces can be obtained by exposure to atomic hydrogen.[10–14] The hydrogen atoms saturate the dangling bonds of the dimer atoms and symmetric dimers consisting of monohydride species are obtained (see Fig. 1). Prolonged exposures of the Ge surface may lead to breaking of the dimer bonds and the formation of a 1×1 surface (probably disordered) with dihydride Ge atoms present, as observed by high-resolution energy-loss spectroscopy.[14]

This paper deals with the electronic structure of both the clean and hydrogen-chemisorbed Ge(001) surfaces investigated by means of photoelectron spectroscopy. Parts of the angle-resolved photoemission (ARPES) results for the valence band of the clean 2×1 surface have been presented earlier. A detailed comparison was made between experimentally and theoretically determined surface-state band structures.[15] Employing the local-density approximation and Green's functions, the surface band structure along the [010] direction was calculated self-consistently for an asymmetric dimer model of the 2×1 reconstructed surface. The comparison was restricted to the [010] direction where the most detailed and clear experimental picture is obtained by ARPES. Dimers on adjacent terraces, separated by monatomic steps, will be oriented in different directions separated by 90°. The (001) surfaces of Ge and Si thus normally con-

0163-1829/94/49(23)/16523(11)/$06.00

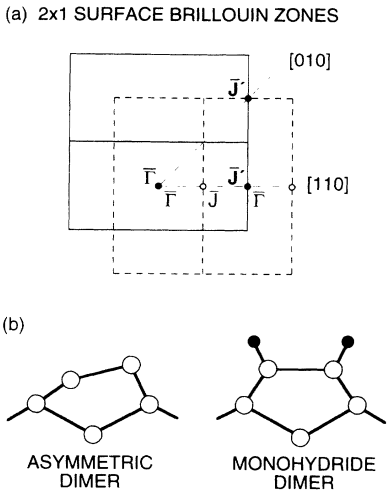

FIG. 1. (a) The surface Brillouin zones for the two perpendicularly oriented 2×1 domains. Surface states along the high-symmetry directions, $\bar{\Gamma}$-$\bar{J}$ and $\bar{\Gamma}$-$\bar{J}'$, are superimposed in ARPES spectra recorded along the [110] direction, while equivalent $\bar{k}_{\parallel}$ points of the domains are probed along the [010] direction. (b) Models of the asymmetric dimer of the clean surface and the symmetric dimer of the monohydride surface.

sist of domains with their 2×1 surface Brillouin zones (SBZ's) oriented perpendicular to each other (see Fig. 1). The electronic structure along the $\bar{\Gamma}$-$\bar{J}$ and $\bar{\Gamma}$-$\bar{J}'$ lines is therefore superimposed in ARPES spectra recorded along $\langle 110 \rangle$ directions. In the [010] direction one probes equivalent $\bar{k}_{\parallel}$ points in the two SBZ's and thereby one avoids ambiguities due to the differently oriented domains.

In this paper surface-state dispersions for the Ge(001)2×1 and Ge(001)2×1:H surfaces along the [010], as well as the [110] direction, are presented in order to give a more complete picture of the surface-state bands and to study the effect of hydrogen chemisorption on the surface electronic structure. The study of the 2×1:H surface, which is very interesting in itself, has been valuable when interpreting the data from the clean surface. The sensitivity to hydrogen chemisorption is an almost ideal test for surface-state identification on the clean 2×1 surface. The surface umklapp scattering of bulk structures will not be sensitive to the hydrogen, since the periodicity of the surface remains the same. In addition, high-resolution core-level spectroscopy and ARPES results for the Ge(001) 2×1 to $c(4\times2)$ phase transition are presented and discussed.

II. EXPERIMENTAL DETAILS

The experiments were performed at two different synchrotron-radiation facilities. The valence-band electronic structure of the clean 2×1 and the monohydride 2×1:H surfaces was studied at HASYLAB, DESY, Germany using the polarized synchrotron radiation from the DORIS II storage ring and a VG ADES 400 spectrometer. The angle-resolved photoemission spectra were recorded for different emission angles at mainly two photon energies (14 and 17 eV) for the two surfaces. The total-energy resolution was ~0.18 eV and the angular resolution $\sim2°$ in those measurements. Spectra were recorded with three different experimental geometries in order to investigate the polarization dependence of the surface states. For normal incidence of the light ($\theta_i=0°$) the electric-field vector was either in the plane defined by the surface normal and the emission direction of the measured photoelectrons, or perpendicular to the same plane. These geometries will be referred to as the $A_{\parallel}$ and $A_{\perp}$ cases, respectively. Most of the spectra shown in this paper were recorded with $\theta_i=45°$ and the polarization according to the $A_{\parallel}$ case. Normal-emission spectra, at photon energies from 8 to 27 eV, were also measured for the 2×1:H surface in order to study the bulk valence-band structure.

At the MAX Synchrotron Radiation Laboratory in Lund, Sweden, the room-temperature 2×1 and the low-temperature $c(4\times2)$ reconstructions of the clean Ge(001) surface were studied. The sample holder allowed cooling of the sample down to a temperature of ~120 K. Using the toroidal-grating monochromator beamline and an angle-resolving VSW ARIES hemispherical analyzer both Ge $3d$ core-level and valence-band spectra were recorded.

The sample was an n-type ($\rho\sim10$ mΩ cm, Sb doped), mirror polished, Ge(001) crystal. A clean, two-domain, 2×1 surface was prepared by Ar-ion sputtering followed by resistive heating up to 600–800 °C, which resulted in a well-defined 2×1 LEED pattern at RT. A sharp $c(4\times2)$ LEED pattern was obtained when the sample was cooled. Traces of half-order streaks could be observed in the background of both the 2×1 and $c(4\times2)$ LEED patterns, in agreement with other studies (see, for instance, the LEED patterns shown in Ref. 6). The hydrogen exposure was done with the Ge surface facing a hot (~1700 °C) tungsten filament at a distance of ~10 cm. An exposure of 750 L gave rise to a diffuse 2×1 LEED pattern. The sample was then annealed ~30 s at a temperature below 300 °C, the temperature at which hydrogen desorbs from Ge(001).[14] After that, a well-defined 2×1 LEED pattern was obtained. The Fermi-level position (E_F) was determined by photoemission from the metallic (TA) sample holder. In order to calculate the $\bar{k}_{\parallel}$ values the necessary work functions were determined from the low-energy cutoff in the photoemission spectra. The values 4.7 and 4.5 eV have been used for the clean and 2×1:H samples, respectively.

III. VALENCE-BAND RESULTS

In Figs. 2 and 4 ARPES spectra recorded at RT from the clean Ge(001)2×1 surface are shown for different emission angles in the [010] and [110] directions. The corresponding set of spectra for the monohydride Ge(001)2×1:H surface is shown in Figs. 3 and 5. The $E(\bar{k}_{\parallel})$ dispersions obtained from these and other spectra are plotted in Figs. 6–9 together with the calculated projected bulk band structure (shaded area) in the [010] and [110] directions from Refs. 15 and 9, respectively. In the figures for the clean surface (Figs. 6 and 8) the calculated surface-state bands from these references are included.

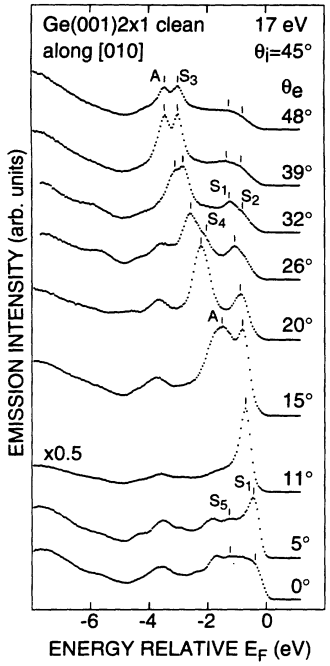

FIG. 2. Angle-resolved valence-band spectra obtained from the clean Ge(001)2×1 surface, with 17-eV photon energy, at various emission angles θ_e along the [010] direction. Structures S_1–S_5 are interpreted as surface states and structure A as due to a direct bulk transition.

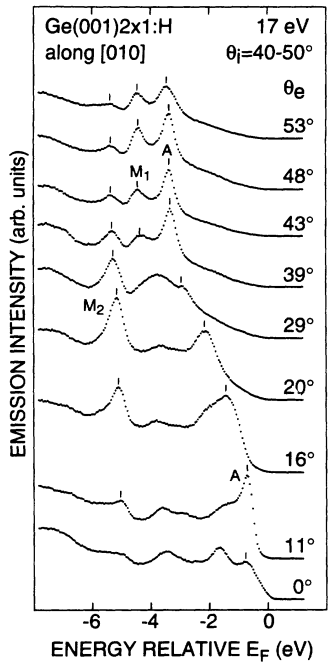

FIG. 3. Angle-resolved valence-band spectra obtained from the hydrogen-chemisorbed Ge(001)2×1:H surface, with 17-eV photon energy, for various emission angles θ_e along the [010] direction. Structures M_1 and M_2 are interpreted as hydrogen-induced surface states.

Due to improvements introduced in the calculations performed for the [010] direction,[15] the surface-state bands were found ~0.2 eV higher up in energy than in the calculation along the high-symmetry directions.[9] The calculated surface bands plotted in Fig. 8 have been shifted in energy in order to obtain the same energy at the symmetry points $\bar{\Gamma}$ and $\bar{J}'$ as for the corresponding bands in Fig. 6. The same value 0.3 eV, as in Ref. 15 has been used for the difference between the experimentally determined Fermi level and the valence-band maximum E_V in the calculation. This value was chosen in order to get the best agreement between the experiment and theory for the surface-state bands along the [010] direction. Since the energy shift of the bulk features in the spectra after hydrogen chemisorption was almost negligible (within 0–0.1 eV towards lower binding energy), $E_F - E_V = 0.3$ eV was also used for the 2×1:H surface (Figs. 7 and 9).

Five surface-related structures S_1–S_5 are identified in the photoemission spectra of the clean Ge(001)2×1 surface in the [010] direction (Fig. 2). They are all sensitive to hydrogen chemisorption (compare with the 2×1:H spectra in Fig. 3) and their energy dispersions $E(\bar{k}_\parallel)$ are independent of the photon energies used in the experiment. One strong structure A is almost entirely unaffected by the presence of hydrogen on the surface and is interpreted as due to a direct bulk transition. Strictly speaking, surface features within the projected bulk band structure are actually surface resonances. However, in the following discussion all surface features are for simplicity called surface states.

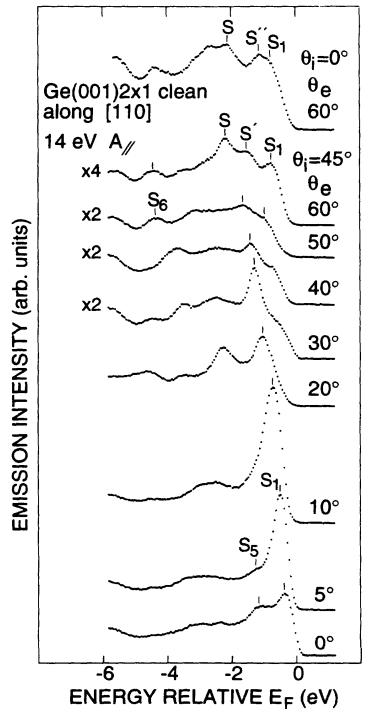

FIG. 4. Angle-resolved valence-band spectra obtained from the clean Ge(001)2×1 surface, with 14-eV photon energy, for various emission angles θ_e along the [110] direction. The uppermost spectrum was recorded with normal incidence of the light ($\theta_i = 0°$).

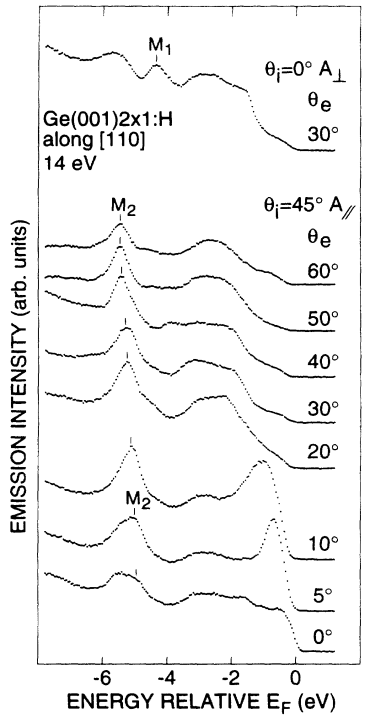

FIG. 5. Angle-resolved valence-band spectra obtained from the hydrogen-chemisorbed Ge(001)2×1:H surface, with 14-eV photon energy, for various emission angles θ_e along the [110] direction. The uppermost spectrum was recorded with normal incidence of the light ($\theta_i=0°$) and the electric-field vector perpendicular to a plane defined by the [001] and [110] directions, in order to illustrate the polarization dependence for the hydrogen-induced surface states M_1 and M_2.

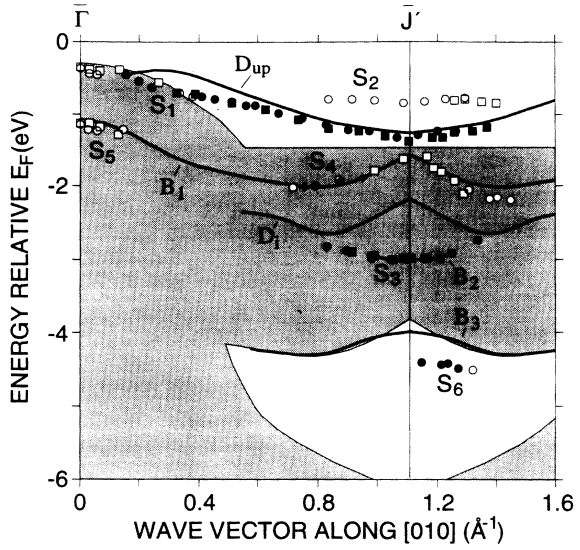

FIG. 6. Experimental surface-state dispersions for the clean Ge(001)2×1 surface (S_1–S_5) along the [010] direction. Data points, obtained with 17-eV (●) and 14-eV (■) photon energy, are shown for $\theta_i=45°$. Open symbols denote weak surface structures or surface structures overlapping with direct bulk transitions. Data points obtained for normal incidence ($\theta_i=0°$) at 17-eV (◆) photon energy are also included for the state S_4. Calculated surface-state bands (D_{up}–B_3) and the projected bulk band structure (shaded area) from Ref. 15 are included. The valence-band maximum is positioned 0.3 eV below E_F in order to align the calculated and experimental bands.

In normal emission spectra the surface-state contribution is rather weak. A comparison between 2×1 and 2×1:H spectra reveals, however, two clear surface-state features for the clean surface, S_1 and S_5, located at about 0.3–0.4 and 1.15 eV below E_F (compare the $\theta_e=0°$ spectra in Figs. 2–5). While S_5 only can be observed close to $\bar{\Gamma}$, S_1 can be followed in all the spectra in Fig. 2. It disperses downwards from −0.4 eV at $\bar{\Gamma}$ to −1.35 eV at $\bar{J}'$ ($\theta_e=39°$). For some emission angles S_1 overlaps with the direct bulk transition A, but the surface-state contribution can be determined by comparisons with the 2×1:H spectra in Fig. 3. Note, for instance, the very strong peak in the $\theta_e=11°$ spectra, which is reduced to a much less intense, but still clear, peak after hydrogen chemisorption. The overlap with bulk structures is indicated by open symbols in the dispersion for S_1 in Fig. 6.

The structure S_3 appears as a sharp and pronounced peak in the spectra and has a minimum in the initial-state energy of 3.0 eV below E_F at the $\bar{J}'$ point ($\theta_e=48°$). Going from $\bar{J}'$ towards $\bar{\Gamma}$ in the SBZ, S_3 can be followed until it starts to overlap with the dispersive bulk structure A. Both S_3 and S_1 are suppressed when changing the incidence angles from 45° to 0°, indicating a dominating p_z character for these states.

Structure S_4 disperses upwards to an initial energy of

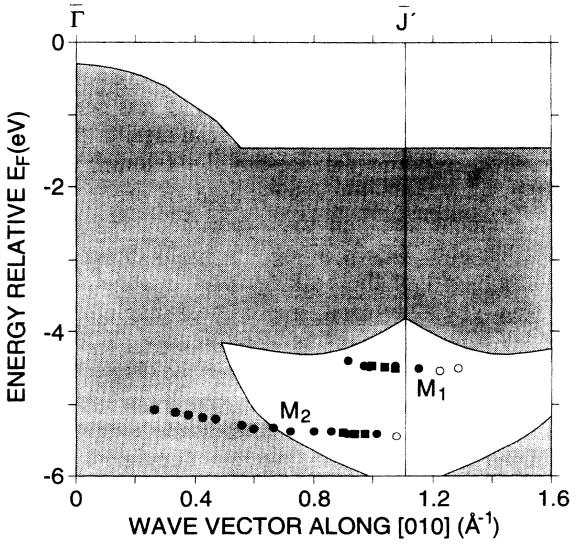

FIG. 7. Experimental surface-state dispersions for the hydrogen-chemisorbed Ge(001)2×1:H surface (M_1 and M_2) along the [010] direction. Data points, obtained with 17-eV (●) and 14-eV (■) photon energy are shown for $\theta_i=45°$. Open symbols denote weak structures. A value of $E_F-E_V=0.3$ eV is used for the position of the projected bulk band structure (shaded area).

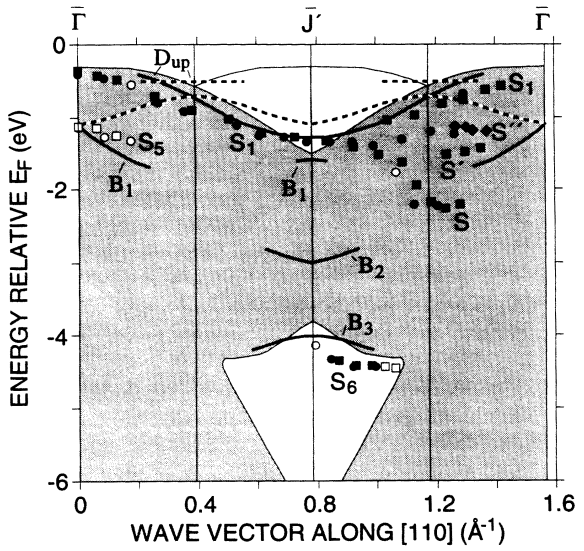

FIG. 8. Experimental surface-state dispersions for the clean Ge(001)2×1 surface (S_1–S_5) along the [110] direction. Data points, obtained with 17-eV (●) and 14-eV (■) photon energy, are shown for $\theta_i=45°$. Open symbols denote weak surface structures or surface structures overlapping with direct bulk transitions. Data points obtained for normal incidence ($\theta_i=0°$) at 14-eV (◆) photon energy are also included in the figure for the state S''. Calculated surface-state bands, along $\bar{\Gamma}$-$\bar{J}'$-$\bar{\Gamma}$ and $\bar{\Gamma}$-$\bar{J}$-$\bar{\Gamma}$-$\bar{J}$-$\bar{\Gamma}$, from Ref. 9 are indicated by full and dashed lines, respectively, together with the projected bulk band structure along these directions (dark and light shading).

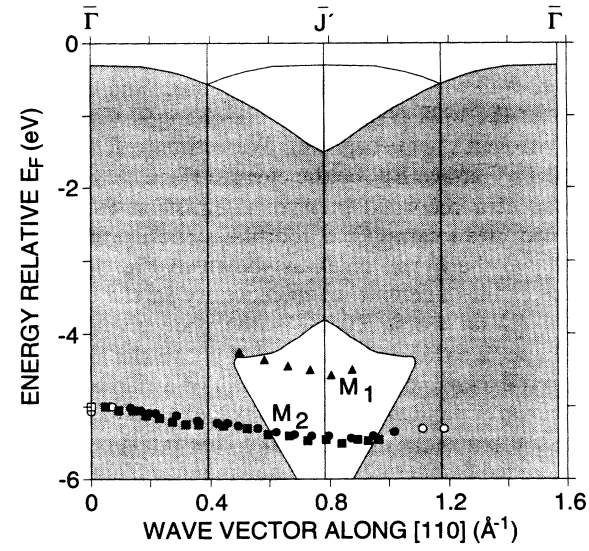

FIG. 9. Experimental surface-state dispersions for the hydrogen-chemisorbed Ge(001)2×1:H surface (M_1 and M_2) along the [110] direction. Data points, obtained with 17-eV (●) and 14-eV (■) photon energy, are shown for $\theta_i=45°$ together with data points obtained for normal incidence ($\theta_i=0°$) and the electric-field vector perpendicular to a plane defined by the [001] and [110] directions at 14-eV (▲) photon energy.

~ -1.6 eV at $\bar{J}'$. An accurate determination of the energy position at this point is difficult, due to the interference with the structure S_1. S_4 is a rather weak structure in the spectra obtained with an angle of incidence of 45°, but becomes more pronounced in the spectra with normal incidence (shown in Fig. 2 in Ref. 15), indicating a higher degree of p_x-p_y character compared to the other structures. Another structure S_2 is observed well above the projected bulk bands, at ~ 0.8 eV below E_F, around $\bar{J}'$. The S_2 state is a weak feature seen only as a shoulder in the spectra. No significant dispersion of this state could be determined.

All features observed above structure A around $\bar{J}'$ in the [010] direction are totally removed in the spectra recorded after the hydrogen chemisorption (Fig. 3). Instead two new strong structures M_1 and M_2, dispersing downwards when going towards $\bar{J}'$ ($\theta_e\sim 53°$), are observed. As can be seen in Fig. 7 these structures appear around $\bar{J}'$ in a bulk band gap, at initial energies of -4.5 and -5.5 eV, respectively, which clearly separates them from the bulk electronic structure.

A comparison of the dispersions of measured and calculated bands shown in Fig. 6 leads to an identification of S_1 with the dangling-bond band D_{up}, of S_3 with the back-bond state B_2 and of S_4-S_5 with the back-bond state B_1. The different characters of the theoretical bands are discussed in detail in Refs. 15 and 16 and they are found to be consistent with the experimentally observed p_z character for S_1 and S_3 and the p_x-p_y character of S_4. The relative energy positions and dispersions for the calculated bands are in excellent agreement with experiment. Only the surface state S_2 remains unexplained by the calculated surface band structure.

In the [110] direction the situation is more complicated, due to the fact that one simultaneously probes $\bar{\Gamma}$-$\bar{J}'$ and $\bar{\Gamma}$-$\bar{J}$-$\bar{\Gamma}$ directions in the SBZ's corresponding to the two perpendicular domains. Structures in the spectra are, due to this, more difficult to separate and to interpret unambiguously. In the clean 2×1 spectra shown in Fig. 4, S_1 can be followed from $\theta_e=0°$ up to $\theta_e=30°$ corresponding to a $\bar{J}'$ point for one of the domains. For higher emission angles several structures are observed between -2.5 eV and E_F. The upper structure is labeled S_1 in order to obtain symmetry around $\bar{J}'$ for this state. S and S' are observed at -2.15 and -1.5 eV, respectively, for $\theta_e=60°$. When changing the geometry of the experiment from $\theta_i=45°$ to normal incidence, S' disappears and another structure S'' shows up at -1.15 eV (uppermost spectrum in Fig. 4).

At ~ 4.4 eV below E_F a possible surface-state candidate S_6 can be observed for some emission angles in the [110] direction. The structure disappears in the corresponding 2×1:H, spectra while in the spectra recorded with the $A_\perp$ geometry the hydrogen-induced state M_1 shows up at this energy. S_6 can also be observed with 17-eV photon energy at the same energy, supporting an interpretation as a surface state. A structure remains, however, for $h\nu=17$ eV, also after hydrogen chemisorption. This suggests contributions from bulk transitions to S_6, but contributions from the M_1 state due to a nonper-

fect $A_\parallel$ polarization is also possible.

Clear shoulders can be seen at energies above S_1 in the clean 2×1 spectra recorded at $\theta_e=30°$ and 40° in Fig. 4. Structures originating from the dangling bond of the other domain, D_{up} along $\bar{\Gamma}$-$\bar{J}$-$\bar{\Gamma}$, are expected to show up here. As can be seen in Fig. 5, shoulders are also present after the hydrogen exposure, which prevents us from making an accurate determination of the surface-state emission in this region. The shoulders present in the 2×1:H spectra are interpreted as due to surface umklapp scattering (which is not affected by the hydrogen chemisorption since the surface periodicity remains the same). Direct bulk transitions near $\bar{\Gamma}$ can be scattered by a surface reciprocal-lattice vector in the $\bar{\Gamma}$-$\bar{J}$-$\bar{\Gamma}$ direction to the vicinity of $\bar{\Gamma}$ in the second SBZ of that domain.[11]

After the hydrogen chemisorption, the hydrogen-induced surface state M_2 is seen with high intensity for almost all the spectra along the [110] direction recorded with $\theta_i=45°$ and the $A_\parallel$ geometry (see Figs. 5 and 9). M_2 disperses downwards from -5 eV close to $\bar{\Gamma}$ to -5.5 eV at $\bar{J}'$ ($\theta_e=50°$). The uppermost spectrum in Fig. 5 was recorded with normal incidence and the $A_\perp$ geometry. As can be seen, the emission from the hydrogen-induced surface states is highly dependent on the polarization of the light. M_1 which could not be observed with $A_\parallel$ shows up as a clear peak with $A_\perp$, while M_2 instead is suppressed with this polarization.

The experimental dispersion of S_1 in the [110] direction is well reproduced by the calculated D_{up} dangling-bond band along $\bar{\Gamma}$-$\bar{J}'$ (full line) in Fig. 8. At some emission angles the back bond B_1 along the $\bar{\Gamma}$-$\bar{J}$-$\bar{\Gamma}$ direction (corresponding to emission from the other domain and indicated by a dashed line in Fig. 8) can possibly contribute to S_1. The surface structure S_5 close to $\bar{\Gamma}$ corresponds well to B_1 in the $\bar{\Gamma}$-$\bar{J}'$ direction. The S' and S'' structures, observed for large emission angles with $\theta_i=45°$ and 0°, respectively, can in principle be explained by the dispersions of B_1 in the $\bar{\Gamma}$-$\bar{J}'$ and $\bar{\Gamma}$-$\bar{J}$-$\bar{\Gamma}$ directions. We cannot, however, explain why a changed incidence angle of the light should result in emission from the other domain. The dispersion of S_6 appears close to another back-bond band B_3, which is a further support for a surface-state assignment for this state. Bulk contributions for certain photon energies cannot, however, be excluded. The valence-band edge follows the dispersion of B_3 closely, which makes it difficult to distinguish between emission from B_3 and from bulk states. We cannot securely deduce whether S_6 is due to bulk or surface origins or a combination. Note, also, that after hydrogen chemisorption M_1 appears in the same energy range as S_6 for the clean surface, but then only for the $A_\perp$ polarization of the light. A correspondence to S cannot be found in the calculated band structure.

In the hydrogen-chemisorbed normal-emission spectra recorded with 14-eV photon energy there is still some emission close to the Fermi level ($\theta_e=0°$ spectrum in Fig. 5). This is even more apparent in a corresponding spectrum (shown at the top in Fig. 10) recorded with a lower photon energy $h\nu=10$ eV where the emission at the Fermi level looks like a sharp Fermi edge, with a width

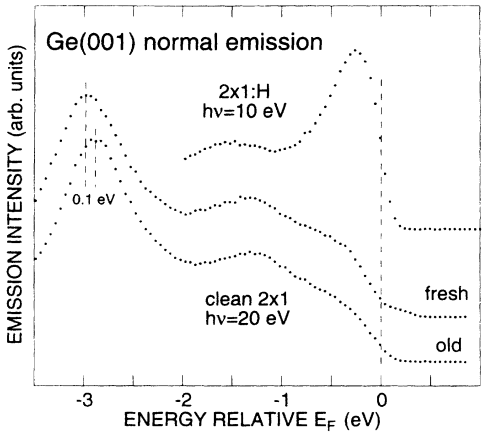

FIG. 10. Angle-resolved valence-band spectra recorded in normal emission illustrating the appearance of the structures close to the Fermi level. At the top is a spectrum recorded with 10-eV photon energy from the hydrogen-chemisorbed 2×1 surface. Below, spectra recorded a few minutes and 2.5 h after annealing of the clean 2×1 surface are compared, in order to show the influence of the time elapsed after cleaning on the small footlike structure located just above the Fermi level.

determined by the experimental resolution. Since the features at the Fermi level are observed only at some special photon energies and also after the hydrogen chemisorption, we interpret these structures as due to direct bulk transitions from the uppermost valence band. From these observations we conclude that the Fermi-level position lies at, or at least very close to, the valence-band maximum for the 2×1:H surface. This is very surprising since the sample is n doped and for the hydrogen-chemisorbed surface, no surface states that can pin the Fermi level are expected in the band gap. The Fermi-level position for the clean 2×1 surface must then also be very close to the valence-band edge, since the binding energies of the bulk structures were changed very little by the hydrogen chemisorption. We estimate E_F to be less than 0.1 eV above E_V for the clean surface.

In spectra recorded in normal emission from freshly annealed clean samples, a footlike structure is observed just above the Fermi level, as shown in Fig. 10. Even if one takes into account an uncertainty in the determination of E_F (at worst ±0.1 eV) the state giving rise to a line shape like this must be located above the Fermi level. Thermal excitation to the minimum of a normally empty surface-state band, located 0.1–0.2 eV above the Fermi level, is a plausible explanation. This interpretation will be discussed further below. The emission from the structure decayed rapidly with time after cleaning. It was suppressed to approximately half the intensity 30 min after annealing the sample. In Fig. 10, spectra recorded a few minutes and 2.5 h after annealing of the sample to ~600 °C are compared. The decrease in intensity is accompanied by a small energy shift ~0.1 eV of the bulk structure, seen at ~-3 eV. Thus, the disappearance of the structure is related to a change in Fermi-level position towards the valence-band maximum, lowering the probability of thermal excitation to the normally empty

state. For a freshy annealed sample the Fermi level would then be located 0.1–0.2 eV above the valence-band maximum and the minimum of the empty state can, from this, be roughly estimated to be located 0.2–0.4 eV above E_V or 0.4–0.7 eV above the surface state S_1. In the calculation by Krüger *et al.*[9] a local minimum is found in the dispersion of an empty dangling-bond band D_{down} at $\bar{\Gamma}$, but a slightly lower energy is found at the $\bar{J}'$ point for this state.

The low-temperature $c(4\times2)$ reconstruction of the clean Ge(001) surface was also studied with ARPES. Spectra were recorded with 21.2 eV along the [010] azimuthal direction. In Fig. 11 the surface-state emission for the surface states S_1–S_3 from the $c(4\times2)$ and 2×1 surfaces is compared. At an emission angle of 34°, $\bar{k}_{\parallel}$ points close to a $\bar{J}'$ ($\bar{J}$) point of the 2×1 [$c(4\times2)$] SBZ are probed. No significant changes could be observed in any of the recorded spectra after cooling the sample to ~120 K. The valence-band electronic structure of the 2×1 and $c(4\times2)$ surfaces seems to be very similar.

IV. CORE-LEVEL RESULTS AND INTERPRETATIONS

Ge 3*d* core-level spectra were recorded for both the RT, 2×1, and the low-temperature, $c(4\times2)$, reconstructions of the clean Ge(001) surface with photon energies between 38 and 70 eV. In Fig. 12, a 2×1 spectrum recorded at $\theta_e=60°$ is shown together with $c(4\times2)$ spectra recorded at $\theta_e=60°$ and 0°. The 60° emission angle corresponds to a higher surface sensitivity. Apart from a slightly smaller linewidth in the spectra recorded at low temperature, the $c(4\times2)$ and 2×1 spectra look very similar with a surface-sensitive shoulder clearly resolved on the low-binding-energy side of the spectra. In order to investigate the spectra further, a least-squares-fitting procedure in which the spectra were decomposed into components consisting of spin-orbit split Voigt functions was applied. Ge 3*d* core-level spectra from the clean Ge(001) surface have previously been decomposed in three different ways in the literature: (1) one surface component assigned either to up atoms of asymmetric dimers[17] or to almost a full surface layer of covalent dimer atoms;[18] (2) two surface components of which one is shifted towards the right, assigned to a full top layer, and the second is shifted towards the left, assigned to the second layer;[19] (3) two surface components shifted towards lower binding energy, with assignments that will be discussed below.[20,21] We found that by using alternative (3) the best quality was obtained for the fits of individual spectra. Moreover, by using two surface components shifted to the right, consistent fits could be obtained for spectra recorded with different photon energies and emission angles, keeping the energy shifts constant within 0.02 eV, and using reasonable line widths. The decompositions of the spectra are shown by the solid curves in Fig. 12. The parameters used and the obtained core-level shifts and intensities can be found in Table I. For the $c(4\times2)$ spectra the width of the *S* component (0.25 eV) was determined by the shape of the shoulder in the most surface-sensitive spectrum ($\theta_e=60°$). This width was then used for both *S* and *S'* in all $c(4\times2)$ spectra. The best results were obtained when the *B* component was allowed to adopt a Gaussian width slightly larger than for the shifted components. This width could vary between different spectra and were larger in spectra recorded with higher surface sensitivity (compare the $\theta_e=60°$ and 0° spectra in Fig. 12). The obtained shifts relative to the *B* component are -0.51 ± 0.01 eV and -0.18 ± 0.02 for *S* and *S'*, respec-

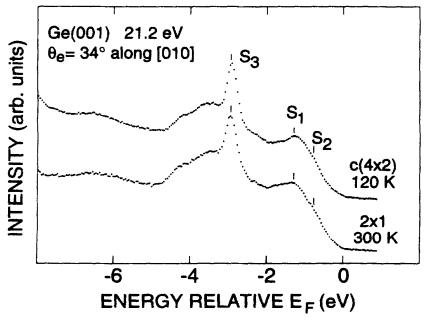

FIG. 11. Comparison of angle-resolved valence-band spectra obtained from the Ge(001) 2×1 and $c(4\times2)$ surfaces. With the 34° emission angle in the [010] azimuthal direction, $\bar{k}_{\parallel}$ points close to a $\bar{J}'$ ($\bar{J}$) point of the 2×1 [$c(4\times2)$] SBZ are probed.

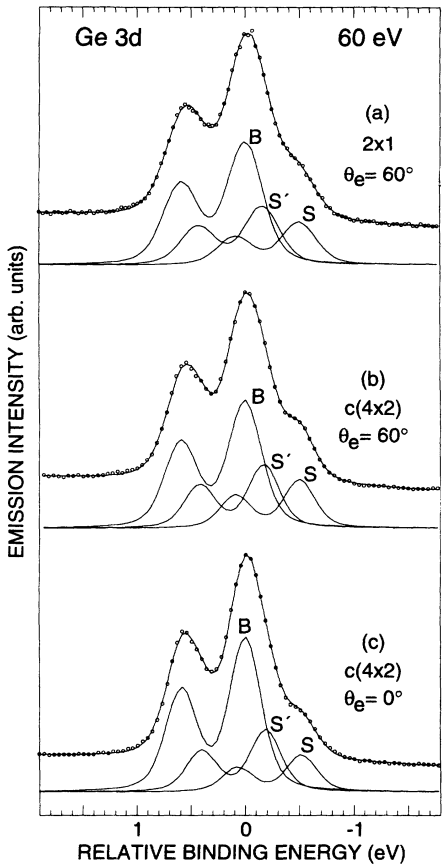

FIG. 12. Ge 3*d* core-level spectra from the 2×1 surface (a) and the $c(4\times2)$ reconstructed surface [(b) and (c)] recorded with 60-eV photon energy. Spectra (a) and (b) are, due to the emission angle of 60°, more surface sensitive than (c) $\theta_e=0°$. Data points are shown by circles and the curves are the result of the curve fitting.

TABLE I. Surface core-level shifts (SCS), fraction of total intensity, and Gaussian width [full width at half maximum (FWHM)] for the different components of the spectra in Fig. 12. A Lorentzian width of 140 meV (FWHM), a spin-orbit split of 590 meV, and a linear background was used in the fitting procedure.

Spectrum	Component	SCS (eV)	Intensity	Width (eV)
(a)	B	0	0.55	0.31
2×1, 300 K	S'	−0.16	0.26	0.30
60 eV, 60°	S	−0.50	0.19	0.30
(b)	B	0	0.54	0.28
$c(4\times2)$,120 K	S'	−0.17	0.26	0.25
60 eV, 60°	S	−0.50	0.20	0.25
(c)	B	0	0.61	0.26
$c(4\times2)$, 120 K	S'	−0.19	0.24	0.25
60 eV, 0°	S	−0.52	0.14	0.25

tively. Except for slightly smaller shifts, our results are in good agreement with the results of Le Lay *et al.*[20] and the results of Cao and co-workers.[21] The component that exhibits the largest shift S is, like in our core-level study of the Si(001) surface,[2] assigned to emission from the up atoms of the asymmetric dimers. In a study of the Ge(001) 2×1 to $c(4\times2)$ and 2×1 to 1×1 phase transitions, Le Lay *et al.* also assigned the component with the largest shift to the up atoms.[20] In addition, they assumed that the corresponding down atoms were contributing to the larger component with the smaller shift (corresponding to S' in this study). Cao and co-workers provided convincing evidence, in their papers,[21] for S' as due to the second-layer atoms. With one layer of Sb dimers substituting the Ge dimers in the top layer, their S component disappeared, while the S' component remained almost unaffected.

A model with S due to the up atoms of the asymmetric dimers, S' solely due to second-layer atoms, and the down atoms contributing to the B component is in best agreement with the intensities of the components obtained from the curve fitting of our data. Considering the $c(4\times2)$ spectrum obtained with $\theta_e=0°$, the intensity of the S component assigned to half the top layer gives an escape depth λ of 4.2 Å. The expected intensities (fractions of total intensity) for the second layer and for the down atoms, together with all atoms below the second layer, calculated using this λ, are then 0.20 and 0.65, respectively, which is in nice agreement with 0.24 and 0.61 observed for S' and B. Calculating the corresponding expected intensities for $\theta_e=60°$, using the intensity of S in that spectrum, one obtains 0.24 and 0.56, which agrees well with the observed values of 0.26 and 0.54, for S' and B, respectively. A perfect correspondence in this kind of intensity considerations cannot be expected, since the intensities of the components are affected by photoelectron diffraction and uncertainties introduced in the curve-fitting procedure. The method should, however, be reliable enough to distinguish between the different candidates for the down-atom emission. If both the down atoms and the second-layer atoms had similar core-level shifts, the S' component would, in the spectra recorded with $\theta_e=60°$, be expected to have a larger intensity than the B component. Our assignment with S due to the up atoms and the down atoms contributing to the B component is also in agreement with a recent core-level study of NH_3 and H_2O adsorption on Ge(001).[22] Adsorbate-induced changes in the spectra revealed a second dimer-atom component overlapping with the bulk contribution.

The B component in the most surface-sensitive $c(4\times2)$ spectrum ($\theta_e=60°$) has a larger linewidth compared to the surface components and the B component in the spectrum recorded with $\theta_e=0°$. This points to the presence of an unresolved surface-shifted contribution close to B, in agreement with the assignments made above. When the linewidth is determined by the vibrational broadening, the bulk component is expected to be narrower than the surface components due to enhanced vibrational broadening from the surface.[23] The larger linewidth for the surface components at RT compared to 120 K, which is the only significant difference between the 2×1 and $c(4\times2)$ spectra, can be explained by a larger vibrational phonon broadening at room temperature and/or a larger amount of disorder for the 2×1 surface.

The results presented here for the Ge 3*d* core level of the Ge(001) surface have many similarities with the Si 2*p* core level of the Si(001) surface.[2] During the phase transition from $c(4\times2)$ to 2×1 the core-level shifts and intensities of the components remain almost unaffected for both surfaces.[2,20] The up atoms give rise to components shifted ~0.5 eV towards lower binding energies and the down-atom components are located close to the bulk line. The component S' associated with the second-layer atoms, on the other hand, is shifted ~0.2 eV towards higher binding energy for Si(001), which is in the opposite direction compared to Ge(001) where the shift is ~0.18 eV toward lower binding energies. The surface core-level shifts of Si(001) and Ge(001) have very recently been theoretically investigated by Pehlke and Scheffler.[24] By calculating the core-level shifts from differences of total energies of slabs containing excited atoms at different positions at the surface and in the bulk, final-state screening effects could be taken into account. Core-level shifts, calculated with initial-state theory alone and with final-state theory, were compared with our experimental results (Ref. 2 and this work). It was shown that for the Si(001) and Ge(001) surfaces, final-state effects have a large influence on the core-level shifts for the different atoms. Pehlke and Scheffler[24] found an enhanced core-hole screening at the surface that was larger for the down atoms than for the up atoms of the dimer.

V. DISCUSSION OF THE CLEAN SURFACE

Most of the previous ARPES studies of the Ge(001) surface have been mainly concentrated on the bulk electronic structure studied by means of normal-emission spectra recorded at different photon energies.[25–28] Nelson *et al.*[25] also observed two surface states in normal emission, corresponding to the structures labeled S_1 and S_2 in our study. As pointed out by Hsieh, Miller, and

Chiang,[26] there are bulk contributions interfering with the surface structures for some photon energies (which also can be seen in our study and the studies by Chen, Ranke, and Schröder-Bergen[27] and Kipp, Manzke, and Skibowski[28]), making the identification of the surface emission difficult. The amount of surface-state contribution in our spectra can, however, be revealed by a comparison with the corresponding 2×1:H spectra.

The surface band gap at different high-symmetry points of the 2×1 SBZ's was addressed in a combined ARPES and inverse photoemission study by Kipp, Manke, and Skibowski.[29] The presented ARPES results for the occupied surface bands were in good agreement with energies calculated by Krüger *et al.* and with our experimental results, presented here and in Ref. 15, for all symmetry points except $\bar{\Gamma}$. In high-resolution spectra recorded at $\bar{\Gamma}$, a structure interpreted as the $D_{\rm up}$ band was observed 0.27 eV above E_V. The valence-band maximum (E_V) was determined by the maximum peak position of the uppermost bulk band to be located 0.30 eV below E_F. Both these observations were made in spectra recorded with photon energies close to 14 eV (see also Figs. 2 and 4 in Ref. 28). We question these results and suggest an alternative interpretation of those spectra. By letting the structure close to E_F instead be due to a transition from the uppermost bulk band and the structure 0.3 eV below E_F be due to $D_{\rm up}$, a picture is obtained that is consistent, not only with the other normal-emission spectra presented by Kipp, Manzke, and Skibowski[28] (in spectra recorded with 20–26 eV $D_{\rm up}$ is found 0.3 eV below E_F), but also with our determination of $E_F-E_V<0.1$ eV and the observations made after hydrogen chemisorption in this study. As discussed above, the peak at ~-0.3 eV (S_1) decreased in intensity in our 14-eV spectra while the emission close to the Fermi level was unaffected.

The structure observed just above the Fermi level at $\bar{\Gamma}$ in this study, is interpreted as the minimum of a normally empty, antibonding, dangling-bond band. This is most likely the same structure as the one that was reported by Kevan and Stoffel,[30] in a high-resolution ARPES study, as a metallic surface state. The metallic state was observed only in a very narrow angular region around normal emission. The energy position, contamination sensitivity, and photon energy dependence separate this state from the structure observed with 14- and 10-eV photon energy, that here is interpreted as due to the uppermost valence band. The emission from the metallic state was found by Kevan and Stoffel[30] to slowly disappear as the temperature was lowered from RT to 77 K. This behavior was described as a metal-insulator transition coincident with the transformation of the LEED pattern from 2×1 to $c(4\times2)$. Kevan and Stoffel interpreted the metallic state as a defect dangling-bond state that appeared due to disorder of the $c(4\times2)$ reconstruction, induced by flipping of single dimers. This interpretation was later questioned by Mårtensson, Cricenti, and Hansson,[31] who suggested that the structure was due to emission from the bottom of an almost empty surface-state band in analogy with their results for the Si(001) surface. The Fermi level was, in the spectra reported by Kevan and Stoffel, positioned at the high-energy edge of the metallic peak, which is in disagreement with our results where the structure seen at $\bar{\Gamma}$ is located at an energy position above E_F. With the Fermi level located below the "metallic" state, the results reported by Kevan and Stoffel would be fully consistent with an antibonding dangling-bond band located just above the Fermi level. Population by thermal excitation of a dispersing band with a minimum at $\bar{\Gamma}$ will explain both the temperature dependence and the angular dependence of the emission. The photon energy dependence reported by Kevan and Stoffel is also similar to the photon energy dependence of the antibonding dangling-bond band reported in an inverse photoemission experiment from the Ge(001) surface.[32] A high density of defect states must be present in order to explain the large band bending and the Fermi-level pinning below the empty surface-state band. At a temperature of 100 K, when the occupation of the metallic state was frozen out, Kevan observed an increased population in a state located 150 meV below the former position of the metallic state. It is reasonable to assume that this state could be due to some kinds of defects and that it is important for the pinning of the Fermi-level position on a newly annealed surface. For an old surface, additional defect states might appear at higher binding energies and pin the Fermi level closer to the valence-band maximum. This would explain why the antibonding band is more difficult to observe by ARPES on the Ge(001) surface than on the Si(001) surface.[33,34]

As discussed in a previous section, almost all the experimentally observed surface states for both the 2×1 and $c(4\times2)$ reconstructions can be identified with surface-state bands obtained from a calculation using asymmetric dimers in a 2×1 unit cell. One interesting exception is the weak structure S_2 observed around the $\bar{J}'$ point, which like the other surface states remains unaffected during the phase transition. For the Si(001)2×1 surface a state corresponding to S_2 exists at the same energy.[33,34] The main difference in the surface electronic structure between Si(001) $c(4\times2)$ and 2×1 is the increase in intensity and in dispersion of this state when cooling the sample. This state can be explained in terms of a second dangling-bond band that is present as a result of the doubled surface unit cell for the $c(4\times2)$ reconstructed surface.[34–36] A local short-range antiferromagnetic order of the buckled dimers at room temperature will explain the presence of the second dangling-bond band also on the 2×1 surface. The same arguments will also explain the presence of the two empty, antibonding, dangling-bond bands on Si(001)2×1 with minima at $\bar{\Gamma}$ and $\bar{J}'$, respectively, that have been observed with inverse photoemission[37] and, by using highly n-doped samples, also with ARPES.[31,33] The Si(001)2×1 surface should then be viewed as a disorderd $c(4\times2)$ surface with alternating buckling directions of the asymmetric dimers. The same picture should also be valid for the Ge(001)2×1 surface. The fact that the electronic structure is well explained by the calculation using asymmetric dimers in a 2×1 unit cell should not be taken as evidence for a ferromagnetic arrangement of the buckling directions at RT. The absence of changes in the valence-band spectra upon cool-

ing may, on the contrary, point to a large degree of antiferromagnetic order of the buckling directions and that the Ge(001)2×1 surface at RT is more $c(4\times2)$-like than the Si(001)2×1 surface. This is in agreement with the observation of diffraction intensities at the $\frac{1}{4}$-order positions[5,6,30] and the appearance of asymmetric dimers with alternating buckling directions in STM already at RT for Ge(001).[4]

VI. DISCUSSION OF THE HYDROGEN-CHEMISORBED SURFACE

In a combined theoretical and experimental study, Appelbaum Baraff, Hamann, Hagstrum, and Sakurai[12] studied hydrogen chemisorption on the (001)2×1 surfaces of Si and Ge. Angle-integrated photoemission spectra obtained from the Ge(001)2×1:H surface showed good agreement with the calculated local density of states (LDOS) of a monohydride Si(001)2×1 surface consisting of dimers. Two hydrogen-induced structures were found in the photoemission spectra at −4.3 and −5.1 eV relative to E_F (using a value of 4.5 eV for the work function) in good agreement with our results. The two Si-H bonds per unit cell gave rise to two peaks in the calculated LDOS derived from the bonding and antibonding dangling-bond states of the clean surface. The low-energy and high-energy peaks were found to have even and odd symmetry, respectively, with respect to reflection in the mirror plane between the two hydrogen atoms.

Along high-symmetry directions, selection rules can be used to determine the parity of an initial state with respect to a mirror plane.[38] It is reasonable to assume that the peaks M_1 and M_2 in spectra recorded in the [110] direction correspond to emission along $\bar{\Gamma}$-$\bar{J}'$. At $\bar{J}'$ the structures would appear in a band gap and a stronger surface-state emission can thus be expected for this domain than for the other domain corresponding to $\bar{\Gamma}$-$\bar{J}$-$\bar{\Gamma}$. The shapes of the dispersions also justify this assumption. In spectra recorded with the $A_{\parallel}$ geometry along the $\bar{\Gamma}$-$\bar{J}'$ direction, states that are even, with respect to reflection in the mirror plane containing this direction are probed, while odd states are probed with the $A_{\perp}$ geometry.[11] Since M_1 is excited by the $A_{\perp}$ polarization, and M_2 is excited with $A_{\parallel}$, we conclude that M_1 is odd and M_2 is even, with respect to reflection in the mirror plane between the two hydrogen atoms, in accordance with the theoretical prediction by Appelbaum *et al.*[12] The results for M_1 and M_2, concerning energy dispersions and polarization dependence, are also in agreement with the results for two corresponding states found in an ARPES study of a single-domain Si(001)2×1:H surface.[11]

Cho and Nemanich[39] reported ARPES results for a hydrogen-terminated Ge(001) surface prepared by remote H-plasma exposure. The surfaces exhibited 1×1 or diffuse 2×1 LEED patterns, dependent on the temperature used for the H-plasma exposure. One hydrogen-induced peak was observed at ~5.6 eV below E_F. The presence of only one hydrogen-induced state, with a non-dispersive character, suggests a more disordered surface than the 2×1:H surface studied in this work.

VII. CONCLUSIONS

In summary, the surface-state dispersions of the clean Ge(001)2×1 surface and the hydrogen-chemisorbed Ge(001)2×1:H surface have been studied in detail with angle-resolved photoemission. For the clean 2×1 surface the experimental results were compared with a calculated surface band structure, and an excellent agreement is obtained between experimental dispersions in the [010] direction and a dangling-bond band and two different back-bond resonances. In the [110] direction a surface state which is well described by the dangling-bond band is the dominating structure in the spectra. A weak structure, corresponding to a previously reported metallic state, was observed at the $\bar{\Gamma}$ point just above the Fermi level. Thermal excitation to the minimum of a normally empty dangling-bond band is a plausible explanation of this structure.

Both the valence-band the core-level electronic structure of the RT, 2×1, and the cold, $c(4\times2)$, reconstructions of the Ge(001) surface were found to be very similar, suggesting that the difference between the two phases is restricted to the degree of order. Ge 3*d* core-level spectra recorded from RT, 2×1, and cold, $c(4\times2)$, reconstructed surfaces were decomposed into three components and the origins of the components were determined. The up atoms give rise to a component shifted ~0.5 eV towards lower binding energies and the down atoms contribute to the intensity of the bulk line. The component associated with the second-layer atoms is located between the dimer components and exhibits a shift of ~0.18 eV towards lower binding energies.

On the Ge(001)2×1:H monohydride surface, two strong, hydrogen-induced surface states were observed in the valence-band spectra. Both structures appear around $\bar{J}'$ in a bulk band gap, at initial energies of −4.5 and −5.5 eV, respectively, which clearly separates them from the bulk electronic structure. A large band bending was observed for the *n*-doped samples used in this study and the Fermi level was found to be located close to the valence-band maximum for both the clean and the hydrogen-chemisorbed surfaces.

ACKNOWLEDGMENTS

We would like to thank the staffs at HASYLAB and MAX-lab for their most generous help and support. This work was supported by the Swedish Natural Science Research Council.

*Present address: Department of Synchrotron Radiation Research, Institute of Physics, University of Lund, Sölvegatan 14, S-223 62 Lund, Sweden.

[1]For reviews on earlier work on these surfaces, see G. V. Hansson and R. I. G. Uhrberg, Surf. Sci. Rep. **9**, 197 (1988).

[2]E. Landemark, C. J. Karlsson, Y.-C. Chao, and R. I. G. Uhrberg, Phys. Rev. Lett. **69**, 1588 (1992).

[3]R. A. Wolkow, Phys. Rev. Lett. **68**, 2636 (1992).

[4]J. A. Kubby, J. E. Griffith, R. S. Becker, and J. S. Vickers, Phys. Rev. B **36**, 6079 (1987).
[5]M. J. Cardillo and W. R. Lambert, Surf. Sci. **168**, 724 (1986); W. R. Lambert, P. L. Trevor, M. J. Cardillo, A. Sakai, and D. R. Hamann, Phys. Rev. B **35**, 8055 (1987).
[6]R. J. Culbertson, Y. Kuk, and L. C. Feldman, Surf. Sci. **167**, 127 (1986).
[7]R. Rossmann, H. L. Meyerheim, V. Jahns, J. Wever, W. Moritz, D. Wolf, D. Dornisch, and H. Schulz, Surf. Sci. **279**, 199 (1992).
[8]M. Needels, M. C. Payne, and J. D. Joannopoulos, Phys. Rev. Lett. **58**, 1765 (1987).
[9]P. Krüger, A. Mazur, J. Pollmann, and G. Wolfgarten, Phys. Rev. Lett. **57**, 1468 (1986).
[10]L. S. O. Johansson, R. I. G. Uhrberg, and G. V. Hansson, Surf. Sci. **189/190**, 479 (1987).
[11]L. S. O. Johansson, R. I. G. Uhrberg, and G. V. Hansson, Phys. Rev. B **38**, 13 490 (1988).
[12]J. A. Appelbaum, G. A. Baraff, D. R. Hamann, H. D. Hagstrum, and T. Sakurai, Surf. Sci. **70**, 654 (1978).
[13]Y. J. Chabal, Surf. Sci. **168**, 594 (1986).
[14]L. Papagano, X. Y. Shen, J. Anderson, G. Schirripa Spagnolo, and G. J. Lapeyre, Phys. Rev. B **34**, 7188 (1986).
[15]E. Landemark, R. I. G. Uhrberg, P. Krüger, and J. Pollmann, Surf. Sci. Lett. **236**, L359 (1990).
[16]P. Krüger and J. Pollmann, Prog. Surf. Sci. **35**, 3 (1991).
[17]R. D. Schnell, F. J. Himpsel, A. Bogen, D. Rieger, and W. Steinmann, Phys. Rev. B **32**, 8052 (1985).
[18]D. H. Rich, T. Miller, and T.-C. Chiang, Phys. Rev. Lett. **60**, 357 (1988).
[19]D.-S. Lin, T. Miller, and T.-C. Chiang, Phys. Rev. B **45**, 11 415 (1992).
[20]G. Le Lay, J. Kanski, P. O. Nilsson, U. O. Karlsson, and K. Hricovini, Phys. Rev. B **45**, 6692 (1992).
[21]R. Cao, X. Yang, J. Terry, and P. Pianetta, Phys. Rev. B **45**, 13 749 (1992); X. Yang, R. Cao, J. Terry, and P. Pianetta, J. Vac. Sci. Technol. B **10**, 2013 (1992).
[22]W. Ranke and J. Wasserfall, Surf. Sci. **292**, 10 (1993).
[23]D. M. Riffe, G. K. Wertheim, and P. H. Citrin, Phys. Rev. Lett. **67**, 116 (1991).
[24]E. Pehlke and M. Scheffler, Phys. Rev. Lett. **71**, 2338 (1993).
[25]J. G. Nelson, W. J. Gignac, R. S. Williams, S. W. Robey, J. G. Tobin, and D. A. Shirley, Phys. Rev. B **27**, 3924 (1983); Surf. Sci. **131**, 290 (1983).
[26]T. C. Hsieh, T. Miller, and T.-C. Chiang, Phys. Rev. B **30**, 7005 (1984).
[27]X. H. Chen, W. Ranke, and E. Schröder-Bergen, Phys. Rev. B **42**, 7429 (1990).
[28]L. Kipp, R. Manzke, and M. Skibowski, Proc. SPIE **1361**, 794 (1990).
[29]L. Kipp, R. Manzke, and M. Skibowski, Surf. Sci. **269/270**, 854 (1992).
[30]S. D. Kevan and N. G. Stoffel, Phys. Rev. Lett. **53**, 702 (1984); S. D. Kevan, Phys. Rev. B **32**, 2344 (1985).
[31]P. Mårtensson, A. Cricenti, and G. V. Hansson, Phys. Rev. B **33**, 8855 (1986).
[32]J. E. Ortega and F. J. Himpsel, Phys. Rev. B **47**, 2130 (1993).
[33]L. S. O. Johansson, R. I. G. Uhrberg, P. Mårtensson, and G. V. Hansson, Phys. Rev. B **42**, 1305 (1990).
[34]E. Landemark, C. J. Karlsson, Y.-C. Chao, and R. I. G. Uhrberg, Surf. Sci. **287/288**, 529 (1993).
[35]Y. Enta, S. Suzuki, and S. Kono, Phys. Rev. Lett. **65**, 2704 (1990).
[36]J. E. Northrup, Phys. Rev. B **47**, 10 032 (1993).
[37]L. S. O. Johansson and B. Reihl, Surf. Sci. **269/270**, 810 (1992).
[38]J. Hermanson, Solid State Commun. **22**, 9 (1977).
[39]Jaewon Cho and R. J. Nemanich, Phys. Rev. B **46**, 12 421 (1992).

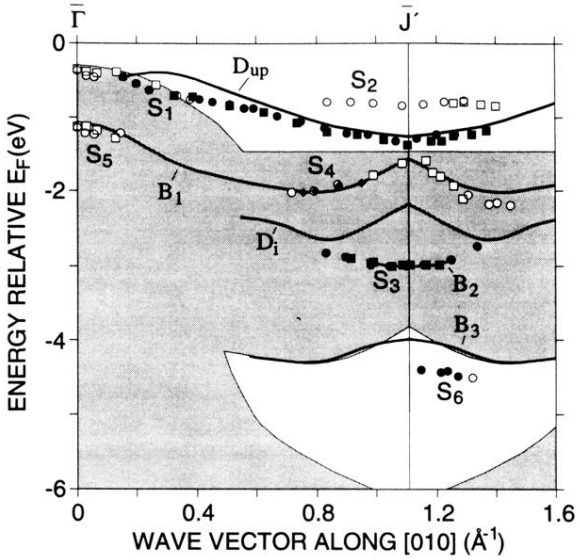

FIG. 6. Experimental surface-state dispersions for the clean Ge(001)2×1 surface (S_1-S_5) along the [010] direction. Data points, obtained with 17-eV (●) and 14-eV (■) photon energy, are shown for $\theta_i=45°$. Open symbols denote weak surface structures or surface structures overlapping with direct bulk transitions. Data points obtained for normal incidence ($\theta_i=0°$) at 17-eV (◆) photon energy are also included for the state S_4. Calculated surface-state bands ($D_{up}-B_3$) and the projected bulk band structure (shaded area) from Ref. 15 are included. The valence-band maximum is positioned 0.3 eV below E_F in order to align the calculated and experimental bands.

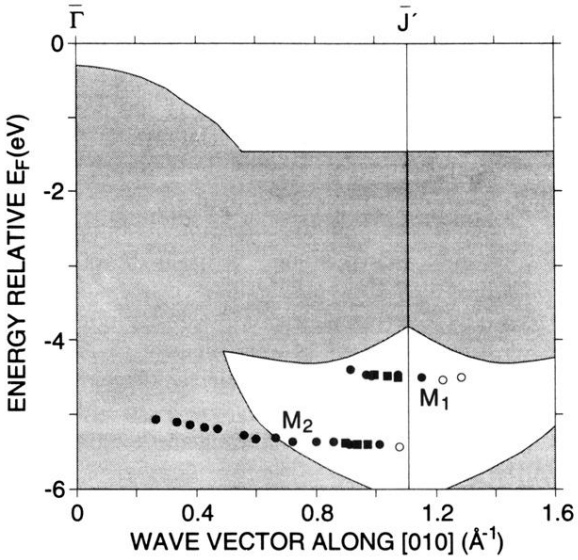

FIG. 7. Experimental surface-state dispersions for the hydrogen-chemisorbed Ge(001)2×1:H surface (M_1 and M_2) along the [010] direction. Data points, obtained with 17-eV (●) and 14-eV (■) photon energy are shown for $\theta_i = 45°$. Open symbols denote weak structures. A value of $E_F - E_V = 0.3$ eV is used for the position of the projected bulk band structure (shaded area).

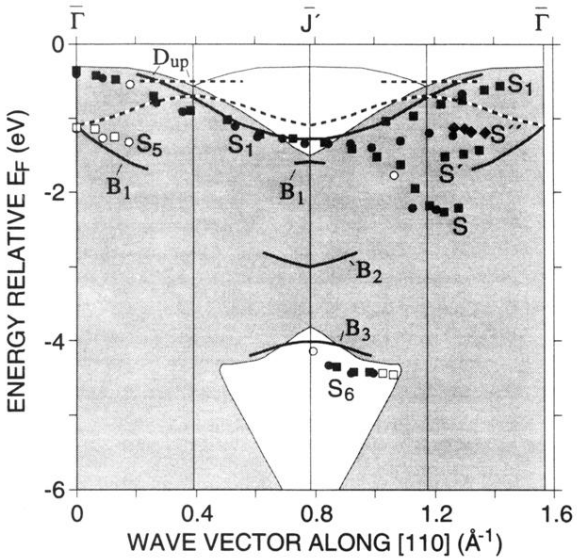

FIG. 8. Experimental surface-state dispersions for the clean Ge(001)2×1 surface (S_1-S_5) along the [110] direction. Data points, obtained with 17-eV (●) and 14-eV (■) photon energy, are shown for $\theta_i=45°$. Open symbols denote weak surface structures or surface structures overlapping with direct bulk transitions. Data points obtained for normal incidence ($\theta_i=0°$) at 14-eV (◆) photon energy are also included in the figure for the state S''. Calculated surface-state bands, along $\bar{\Gamma}$-$\bar{J}'$-$\bar{\Gamma}$ and $\bar{\Gamma}$-$\bar{J}$-$\bar{\Gamma}$-$\bar{J}$-$\bar{\Gamma}$, from Ref. 9 are indicated by full and dashed lines, respectively, together with the projected bulk band structure along these directions (dark and light shading).

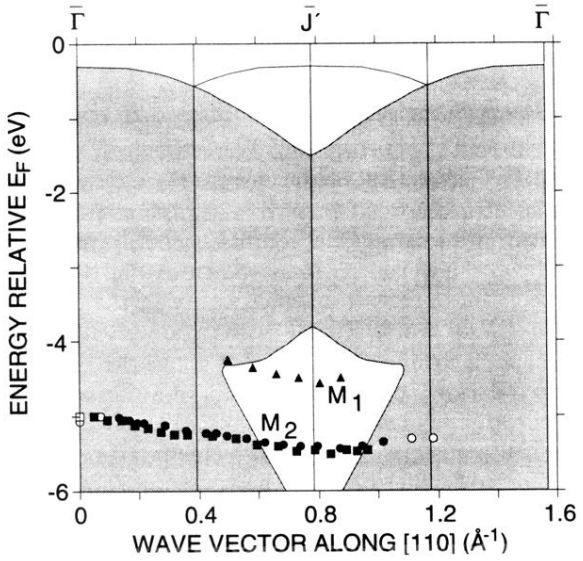

FIG. 9. Experimental surface-state dispersions for the hydrogen-chemisorbed Ge(001)2×1:H surface (M_1 and M_2) along the [110] direction. Data points, obtained with 17-eV (●) and 14-eV (■) photon energy, are shown for $\theta_i = 45°$ together with data points obtained for normal incidence ($\theta_i = 0°$) and the electric-field vector perpendicular to a plane defined by the [001] and [110] directions at 14-eV (▲) photon energy.